arXiv:cond-mat/0105518v1 [cond-mat.stat-mech] 27 May 2001

submitted to
PHYSICAL REVIEW B VOLUME XX, NUMBER XX MONTH XX, YEAR XXXX

Dislocation-induced spin tunneling in Mn_{12} acetate

D. A. Garanin and E. M. Chudnovsky
Department of Physics and Astronomy, Lehman College, City University of New York, 250 Bedford Park Boulevard West, Bronx, New York 10468-1589

(Received 27 May 2001)

Comprehensive theory of quantum spin relaxation in Mn_{12} acetate crystals is developed, that takes into account imperfections of the crystal structure and is based upon the generalization of the Landau-Zener effect for incoherent tunneling from excited energy levels. It is shown that linear dislocations at plausible concentrations provide the transverse anisotropy which is the main source of tunneling in Mn_{12}. Local rotations of the easy axis due to dislocations result in a transverse magnetic field generated by the field applied along the c-axis of the crystal, which explains the presence of odd tunneling resonances. Long-range deformations due to dislocations produce a broad distribution of tunnel splittings. The theory predicts that at subkelvin temperatures the relaxation curves for different tunneling resonances can be scaled onto a single master curve. The magnetic relaxation in the thermally activated regime follows the stretched-exponential law with the exponent depending on the field, temperature, and concentration of defects.

PACS numbers: 75.45.+j, 75.50.Tt

I. INTRODUCTION

Physical properties of Mn_{12} acetate crystals have been subject of intensive investigation in the last years. The crystals have been chemically synthesized by Lis[1] in 1980, who found that they had a centered tetragonal structure with $a = 17.319\mathring{A}$ and $c = 12.388\mathring{A}$ as lattice parameters.[1,2] At the beginning of 1990's Sessoli *et al* of the Florence group of chemists (see, e.g., Refs. 3, 4, 5) established that Mn_{12} clusters located at the sites of the crystal lattice have spin 10. Sessoli *et al* also demonstrated that Mn_{12} crystals are characterized by a record high uniaxial magnetic anisotropy along the c-direction, that makes the 65K energy barrier between the spin-up and spin-down states. The explosion of the interest of physicists to Mn_{12} acetate came after Friedman *et al*[6] measured its spectacular stepwise magnetic hysteresis and explained it by resonant spin tunneling (see also the followup experiments, Refs. 7, 8). Numerous experiments on Mn_{12} performed since 1996 uncovered a number of other interesting phenomena, such as memory effects,[9] non-exponential relaxation,[9,10,11] and a peculiar crossover between thermal and quantum behavior[12,11] predicted by theory.[13,14,15,16,17,18,19,20,21,22,23,24]

Uniaxial spin Hamiltonian, in the field parallel to the anisotropy axis, $\mathcal{H} = -DS_z^2 - H_zS_z$, has pairs of degenerate levels for

$$H_z = kD, \qquad k = 0, \pm1, \pm2, \ldots, \pm(2S-1). \qquad (1)$$

For a sample initially magnetized in the negative z-direction, Mn_{12} molecules occupy spin states with a negative magnetic quantum number m. When the magnetic field is applied in the positive z-direction, the molecules eventually relax to the states with positive m. It may occur via thermal activation over the anisotropy barrier or through quantum tunneling between the states on different sides of the barrier (see Fig. 1). The latter process adds to the thermal activation when the levels on the two sides of the barrier are on resonance, that is, at $H_z = kD$. Consequently, at $H_z = kD$ the magnetic relaxation of the crystal is faster than for the off-resonance values of the field.[6]

There exist two macroscopic experimental approaches to the study of spin tunneling in Mn_{12} (see, e.g., Refs. 6, 7, 8, 25, 26, 27, 28, 29, 10, 9, 30, 11, 12, 31, 32 and references therein). Both clearly demonstrate the effect of resonant spin tunneling. In the first approach, one measures the magnetic relaxation in the crystal at fixed temperature and magnetic field. The theory of such a relaxation works out tunneling transitions between levels on two sides of the energy barrier and spin-phonon transitions between the levels on one side of the barrier. These processes are described by the density-matrix formalism suggested in Ref. 13 and further developed in Refs. 33, 26, 34, 35. In the second approach, one sweeps magnetic field through the resonant value and measures the fraction of molecules that change their magnetic moments. For the ground-state tunneling, the theory of such process has been developed along the lines of the Landau-Zener effect.[36,37,38,39,40,41] A nice feature of the field-sweep approach is that the fraction of molecules that change the direction of the spin depends on the tunneling level splitting and on the sweep rate but is insensitive to the dissipation in the experimental limit of small splitting.

While the uniaxial Hamiltonian allows to compute resonant fields from independent measurements of D, it does not explain why spin tunneling in Mn_{12} actually occurs.

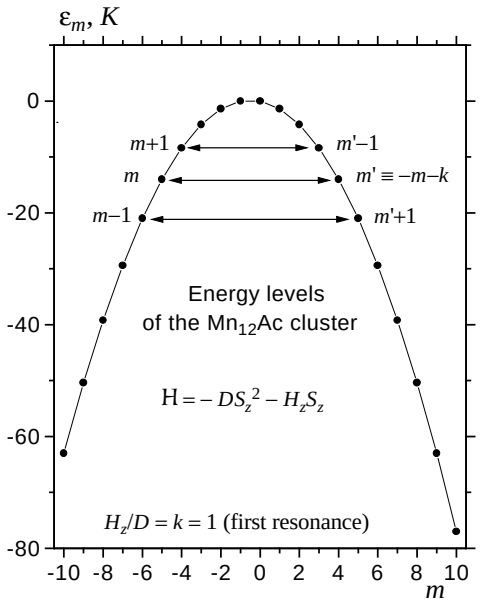

FIG. 1. Spin energy levels of a Mn_{12} Ac molecule for $H_x = 0$ and $H_z = D$ corresponding to the first resonance, $k = 1$.

This is because $\mathcal{H} = -DS_z^2 - H_z S_z$ conserves S_z and thus does not allow any transitions between different m. To obtain tunneling, one should include in the Hamiltonian the terms which do not commute with S_z. The tetragonal symmetry of the crystal does not allow transverse anisotropy terms which are quadratic on the spin operator, i.e., terms proportional to S_x^2 and S_y^2. The lowest order transverse terms must be proportional to $S_+^4 + S_-^4$.[42] If these were the only terms in the Hamiltonian responsible for tunneling, then only resonances with "tunneling length" $m' - m$ (see Fig. 1), which is a multiple of four, would have been observed. This is not the case for Mn_{12}. To explain the presence of resonances with all k, one should invoke a transverse field contribution to the Hamiltonian, $-H_x S_z$. Dipolar fields from magnetic moments of Mn_{12} molecules and hyperfine fields from Mn nuclei have been suggested as natural candidates.[42,13,43,44,45,46,47] Experiments, however, indicate that transverse fields needed to explain the data are stronger than the ones produced by atomic nuclei and magnetic dipoles. The nature of the effects responsible for tunneling in Mn_{12} remains an open question.

Next controversy is the origin of the $\sqrt{t}$ law that approximately fits the initial stage of the relaxation in some experiments.[9,11,32] Suggested explanations include collective effects due to dipolar interaction between Mn_{12} molecules[43] and fluctuating random noise.[48] The first requires some special initial conditions which are not satisfied in experiment[45,46,47] while the second requires certain assumptions about the spectrum of fluctuations.

Another open question is the nature of the "minor species" of Mn_{12} that relaxes faster than the "major species", and is present in all samples studied to date. In the subkelvin temperature range, when the relaxation slows down, the minor species is the main source of the relaxation seen in experiment. Wernsdorfer *et al* attribute that species to the defective sites of the crystal lattice (see Footnote 9 in Ref. 9). On general grounds, it is obvious that defects inside the Mn_{12} clusters cannot account for the minor species. Such defects would strongly modify the spin Hamiltonian, which would result in a significant change of the resonant fields and orders-of-magnitude change of tunneling rates, in contrast with experimental observations.

On the contrary, defects of the tetragonal crystal lattice such as dislocations, which do not change the structure of the cluster, should produce symmetry-violating terms in the Hamiltonian that are responsible for tunneling. Some of these terms are *quadratic* in S_x and S_y. For even k [see Eq. (1)] they produce tunneling in a lower order of the perturbation theory than the transverse-field. In addition, dislocations give rise to local rotations of the easy axis, which for $H_z \neq 0$ results in a *transverse field* that unfreezes resonances with odd k.

Because of the long-range nature of deformations caused by dislocations, the number of affected crystal sites should be relatively large even for a moderate concentration of dislocations. Strong deformations will exist only at a small number of sites inside dislocation cores. Most of the Mn_{12} molecules will develop weak deformations, with the tunneling rate depending on the location of the molecule. Consequently, the relaxation process evolves from the relaxation of the minor species, close to the dislocation cores, to the relaxation of the major species far from the dislocation cores.

In this paper we show that edge and screw dislocations (see Fig. 2) should be the main source of spin tunneling in Mn_{12} crystals. Broad distribution of deformations causes broad distribution of thermal activation and tunneling rates. To study the magnetic relaxation in Mn_{12}, we develop the theory of incoherent Landau-Zener tunneling from excited energy levels. We compute the relaxation law in a crystal with dislocations and show that it obeys scaling that can be tested in experiment. We also demonstrate that in the kelvin temperature range the relaxation is well described by the stretched-exponential law.

The paper is organized as follows. Spin-lattice couplings due to different types of dislocations are studied in Sec. II. Sec. III contains perturbation formulas for the tunneling level splittings for even and odd resonances. The analytical formula for the distribution of transverse anisotropies due to a random array of dislocations is derived in Sec. IV. The distribution of tunnel splittings in Mn_{12} crystals is studied in Sec. V. Sec. VI is devoted to the incoherent Landau-Zener transitions at finite temperatures. In Sec. VII the results are applied to Mn_{12} crystals with the distribution of tunel splittings. In Sec. VIII we compute the magnetic relaxation in the thermal activation regime. The implications of the results obtained in this paper are summarized in Sec. IX.

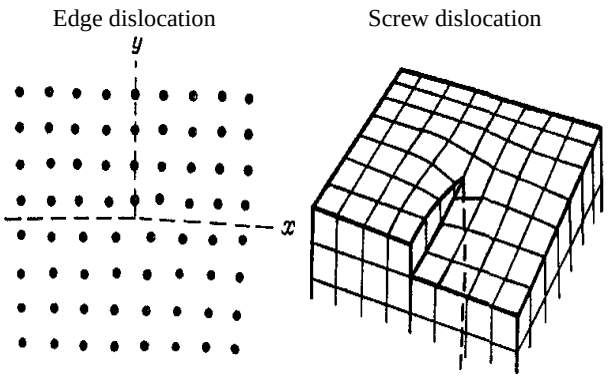

FIG. 2. Edge and screw dislocations.

II. SPIN-LATTICE COUPLINGS DUE TO DISLOCATIONS

A. Spin Hamiltonian

We study the Hamiltonian

$$\mathcal{H} = -DS_z^2 - H_z S_z + \mathcal{H}_{\rm me}, \tag{2}$$

where S_z is the z-component of the spin operator, $S = 10$, $D = 0.65$ K, H_z is the magnetic field applied along the z-axis (c-axis of the crystal), and $\mathcal{H}_{\rm me}$ is the magnetoelastic coupling. The Hamiltonian of Mn_{12} also contains crystal fields of fourth order on the spin operator, magnetic dipole interactions, and hyperfine interactions. We neglect them in order to emphasize the effect of dislocations. The magnetoelastic coupling in Mn_{12} is of the form[42,34,35]

$$\mathcal{H}_{\rm me} = g_1 D(\varepsilon_{xx} - \varepsilon_{yy})(S_x^2 - S_y^2) + g_2 D\varepsilon_{xy}\{S_x, S_y\} + D(\alpha_x\{S_x, S_z\} + \alpha_y\{S_y, S_z\}), \tag{3}$$

where $\{\hat{A}, \hat{B}\}$ is anticommutator,

$$\alpha_x \equiv g_3\varepsilon_{xz} + g_4\omega_{xz}, \qquad \alpha_y \equiv g_3\varepsilon_{yz} + g_4\omega_{yz}, \tag{4}$$

and

$$\epsilon_{\alpha\beta} = \frac{1}{2}\left(\frac{\partial u_\alpha}{\partial x_\beta} + \frac{\partial u_\beta}{\partial x_\alpha}\right), \quad \omega_{\alpha\beta} = \frac{1}{2}\left(\frac{\partial u_\alpha}{\partial x_\beta} - \frac{\partial u_\beta}{\partial x_\alpha}\right) \tag{5}$$

are linear deformation tensors; $\omega_{\alpha\beta}$ being a pure rotation and $\mathbf{u}$ being the displacement. Note that, in principle, the Hamiltonian may contain terms of higher order on deformations. The exact strain tensor also has quadratic contribution on displacement. These terms may become important at and near dislocation cores, that is, for a small number of Mn_{12} molecules which do not contribute much to the relaxation process.

The effect of dislocations is determined by values of constants g_1, g_2,g_3, and g_4. The value of g_4 is fixed by the symmetry of the crystal, $g_4 = 1$.[42,13,49] There are general arguments that all g-constants must be of the same order, see Ref. 50 and references therein. For numerical work we will use $g_1 = g_2 = g_3 = g_4 = 1$.

Before calculating tunneling rates of Mn_{12} molecules due to dislocations, it is convenient to make rotations of the spin axes in (x, y), (x, z), and (y, z) planes in order to transform the Hamiltonian of Eq. (2) into a diagonal quadratic form on spin operators. The terms $\{S_x, S_z\}$ and $\{S_y, S_y\}$ in Eq. (3) are eliminated by rotations by small angles, $\alpha_x/2$ and $\alpha_y/2$, in the (x, z) and (y, z) planes, respectively. This results in a slight renormalization of the uniaxial anisotropy constant D and of the transverse-anisotropy terms. Both effects are quadratic on deformations and are neglected in our approach. The rotations also change the form of the Zeeman term $-H_z S_z$, resulting in the *transverse* field

$$H_\perp \cong \frac{1}{2}\sqrt{\alpha_x^2 + \alpha_y^2}\, H_z \tag{6}$$

in the rotated coordinate system, which is linear on deformations and proportional to the magnetic field H_z applied along the c-axis of the crystal. This transverse field unfreezes tunneling transitions which change the spin projection m by an odd number. The terms $\{S_x, S_y\}$ in Eq. (3) are eliminated by rotations in the (x, y) plane by an angle which is not small. They produce the transverse anisotropy $E(S_{x'}^2 - S_{y'}^2)$ in the first order on deformations.

In the four subsections below, we will consider different types of linear dislocations. We will use formulas of isotropic elastic theory for displacements,[51] which are accurate enough for our conclusions and, at the same time, are less cumbersome than the exact expressions for the tetragonal crystal symmetry. We will see that for all types of linear dislocations the spatial dependence of the transverse anisotropy and the transverse field can be written as

$$E = 2D\frac{g(\varphi)}{r}, \qquad H_\perp = H_z\frac{g_H(\varphi)}{r}, \tag{7}$$

where r is the distance from the dislocation axis, measured in the lattice units, whereas $g(\varphi)$ and $g_H(\varphi)$ are functions of the angle, which are of order one if $g_1 \sim g_2 \sim g_3 \sim g_4 = 1$. One can immediately see from Eq. (7) that the effect of dislocations on tunneling must be strong. Indeed, for $r \sim 1$ one has $E \sim D$, whereas the spatial decay of E is slow, so that each dislocation affects a large number of Mn_{12} molecules in the crystal.

B. Screw dislocation along the anisotropy axis

For screw dislocations shown in Fig. 2 the only nonzero component of the displacement $\mathbf{u}$ is u_z. For the dislocation axis at $x, y = 0$ it is given by

$$u_z(x, y) = \frac{c}{2\pi}\arctan\frac{y}{x}, \tag{8}$$

where c is the lattice spacing along the c-axis. The only nonzero components of deformations are

$$\varepsilon_{xz} = -\omega_{xz} = -\frac{c}{4\pi}\frac{y}{x^2 + y^2}$$
$$\varepsilon_{yz} = -\omega_{yz} = \frac{c}{4\pi}\frac{x}{x^2 + y^2} \tag{9}$$

Thus, according to Eq. (3), screw dislocations along the c-axis do not produce transverse anisotropy of the first order in deformations. They, nevertheless, create a transverse field in the rotated coordinate system, which is given by

$$H_\perp \cong \frac{c}{8\pi}\frac{|g_3 - g_4|}{\sqrt{x^2+y^2}} H_z \tag{10}$$

[cf. Eq. (6)]. This transverse field gives rise to spin tunneling of order $H_\perp^{m'-m}$ between the resonant pair of levels ε_m and $\varepsilon_{m'}$ [see Eq. (2.6) of Ref. 13]. Since $m'-m$ is a usually a large number, this tunneling is much weaker than tunneling due to the transverse anisotropy E from other types of dislocations, which appears in the $E^{(m'-m)/2}$ order for even resonances (see Sec. III for more detail). Since all types of dislocations must be simultaneously present in a crystal, we conclude that c-axis screw dislocations are irrelevant for spin tunneling.

C. Screw dislocation perpendicular to the anisotropy axis

For a screw dislocation along the Y-axis the only nonzero component of the displacement is

$$u_y(x,z) = \frac{b}{2\pi}\arctan\frac{z}{x}, \tag{11}$$

where b is the appropriate lattice spacing. Thus the nonzero components of the deformation tensors are

$$\begin{aligned}\varepsilon_{yz} &= \omega_{yz} = \frac{b}{4\pi}\frac{x}{x^2+z^2}\\ \varepsilon_{xy} &= -\frac{b}{4\pi}\frac{z}{x^2+z^2}.\end{aligned} \tag{12}$$

To bring the spin Hamiltonian to the canonical form, one should first rotate the spin axes in the (y,z) plane by an angle $\alpha_y/2$, which results in a transverse field

$$H_\perp \cong \frac{1}{2}\alpha_y H_z = (g_3+g_4)\frac{b}{8\pi}\frac{x}{x^2+y^2}H_z \tag{13}$$

directed along the new Y-axis. Then the rotation by $\phi = \pi/4$ in the x,y plane transforms $\{S_x, S_y\}$ into $-(S_{x'}^2 - S_{y'}^2)$, which results in the Hamiltonian

$$\mathcal{H} = -DS_{z'}^2 - H_z S_{z'} + E(S_{x'}^2 - S_{y'}^2) - H_{x'}S_{x'} - H_{y'}S_{y'}, \tag{14}$$

where

$$E = -g_2 D\varepsilon_{xy} = g_2 D\frac{b}{4\pi}\frac{z}{x^2+z^2} \tag{15}$$

and

$$H_{x'} = H_{y'} = (g_3+g_4)\frac{b}{8\sqrt{2}\pi}\frac{x}{x^2+y^2}H_z \tag{16}$$

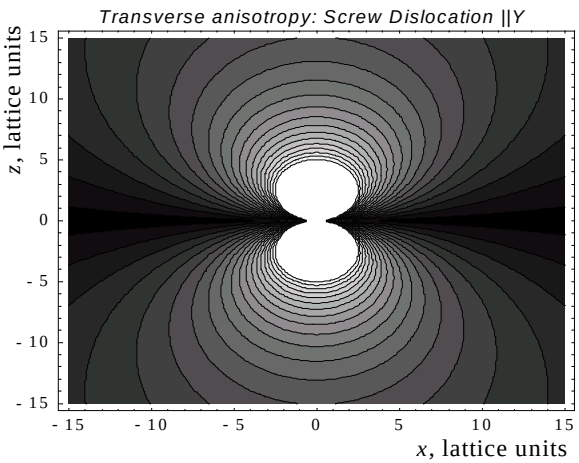

FIG. 3. Contour plot of transverse anisotropy E created by a screw dislocation along the Y-axis, see Eq. (15). (Grey scales are arbitrary.)

(the signs of $H_{x'}$ and $H_{y'}$ are irrelevant). This type of dislocations generates the spatially-dependent transverse anisotropy which is the main source of tunneling. It also generates a transverse field that unfreezes odd resonances. The hard and medium axes, x' and y', interchange when one crosses the plane $z=0$, whereas the transverse field always has equal components along the hard and medium axes.

D. Edge dislocation along the anisotropy axis

For this dislocation shown in Fig. 2 there is no displacement along the c axis, i.e., $u_z = 0$, whereas other displacement components are given by

$$u_x = \frac{b}{2\pi}\left[\arctan\frac{y}{x} + \frac{1}{2(1-\sigma)}\frac{xy}{x^2+y^2}\right] \tag{17}$$

and

$$u_y = -\frac{b}{2\pi}\left[\frac{1-2\sigma}{4(1-\sigma)}\ln(x^2+y^2) + \frac{1}{2(1-\sigma)}\frac{x^2}{x^2+y^2}\right], \tag{18}$$

where $0<\sigma<1/2$ is the Poisson elastic coefficient (we will use $\sigma = 0.25$ in the numerical work). For the deformations one obtains

$$\varepsilon_{xx} - \varepsilon_{yy} = -\frac{b}{\pi(1-\sigma)}\frac{x^2 y}{(x^2+y^2)^2} \tag{19}$$

and

$$\varepsilon_{xy} = -\frac{b}{4\pi(1-\sigma)}\frac{x(x^2-y^2)}{(x^2+y^2)^2}. \tag{20}$$

It is clear that this dislocation does not tilt the anisotropy axis and thus does not generate a transverse field. After the rotation in the (x,y) plane the spin Hamiltonian becomes

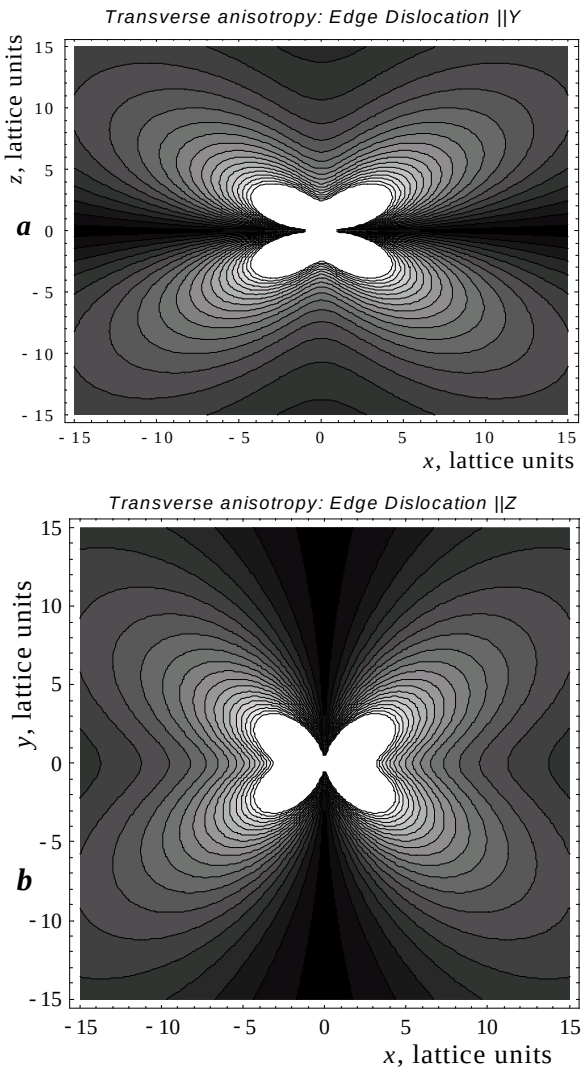

FIG. 4. Contour plots of transverse anisotropy E created by: a - an edge dislocation along the Y-axis, see Eq. (28); b - an edge dislocation along the Z-axis, see Eq. (22).

$$\mathcal{H} = -DS_z^2 - H_z S_z + E(S_{x'}^2 - S_{y'}^2) \tag{21}$$

with

$$E = D\sqrt{g_1^2(\varepsilon_{xx} - \varepsilon_{yy})^2 + g_2^2\varepsilon_{xy}^2}. \tag{22}$$

E. Edge dislocation perpendicular to the anisotropy axis

For such dislocations the nonzero displacements are u_x and u_z. They are given by Eqs. (17) and (18) with $y \Rightarrow z$. For deformations one obtains $\varepsilon_{xy} = 0$,

$$\varepsilon_{xx} - \varepsilon_{yy} = -\frac{b}{4\pi(1-\sigma)} z \frac{(3-2\sigma)x^2 + (1-2\sigma)z^2}{(x^2+z^2)^2} \tag{23}$$

and

$$\alpha_x = \frac{1}{2}\left[(g_3+g_4)\frac{\partial u_x}{\partial z} + (g_3-g_4)\frac{\partial u_z}{\partial x}\right], \tag{24}$$

where

$$\frac{\partial u_x}{\partial z} = \frac{b}{4\pi(1-\sigma)} x \frac{(3-2\sigma)x^2 + (1-2\sigma)z^2}{(x^2+z^2)^2} \tag{25}$$

and

$$\frac{\partial u_z}{\partial x} = \frac{b}{4\pi(1-\sigma)} x \frac{(1-2\sigma)x^2 + (3-2\sigma)z^2}{(x^2+z^2)^2}. \tag{26}$$

The resulting spin Hamiltonian has the form

$$\mathcal{H} = -DS_{z'}^2 - H_z S_{z'} + E(S_{x'}^2 - S_{y'}^2) - H_{x'} S_{x'}, \tag{27}$$

where

$$E = g_1 D(\varepsilon_{xx} - \varepsilon_{yy}), \quad H_{x'} = \frac{1}{2}\alpha_x H_z. \tag{28}$$

Above the XY plane (at $z > 0$) the transverse field is directed along the hard axis, while at $z < 0$ the transverse field is along the medium axis.

III. TUNNEL SPLITTINGS

For concentrations of dislocations upto $c = 10^{-2}$ (in lattice units) most of Mn_{12} molecules are still far from the dislocation cores. Thus the transverse anisotropy and the transverse field generated by dislocations [see, e.g., Eq. (27)] are typically small in comparison with the uniaxial term in the Hamiltonian of the ideal crystal. In this situation one can obtain the tunneling splittings $\Delta_{mm'}$ of resonant pairs of levels in the lowest-order of the perturbation theory. For the model with the transverse field the splittings are[13,52,53]

$$\Delta_{mm'} = \frac{2D}{[(m'-m-1)!]^2} \times \sqrt{\frac{(S+m')!(S-m)!}{(S-m')!(S+m)!}} \left(\frac{H_x}{2D}\right)^{m'-m}. \tag{29}$$

For the transverse anisotropy model, the splittings have been calculated in Ref. 53 for $H_z = 0$ and generalized in Ref. 20 for any field bias. It is convenient to rewrite Eq. (4) of Ref. 20 in the form

$$\Delta_{mm'} = \frac{2D}{[(m'-m-2)!!]^2} \times \sqrt{\frac{(S+m')!(S-m)!}{(S-m')!(S+m)!}} \left(\frac{|E|}{2D}\right)^{(m'-m)/2}. \tag{30}$$

In the transverse-anisotropy model, $\Delta_{mm'}$ is nonzero for even $m'-m = -2m-k$, which for even S requires an even value of the tunneling resonance number k. For odd values of $m'-m$, tunneling resonances are quenched, $\Delta_{mm'} = 0$.

In Mn_{12} samples with dislocations, both the transverse field and the transverse anisotropy are present, see Eq. (7). Since at resonances the longitudinal field satisfies $H_z = kD$, the transverse field is well defined for a given

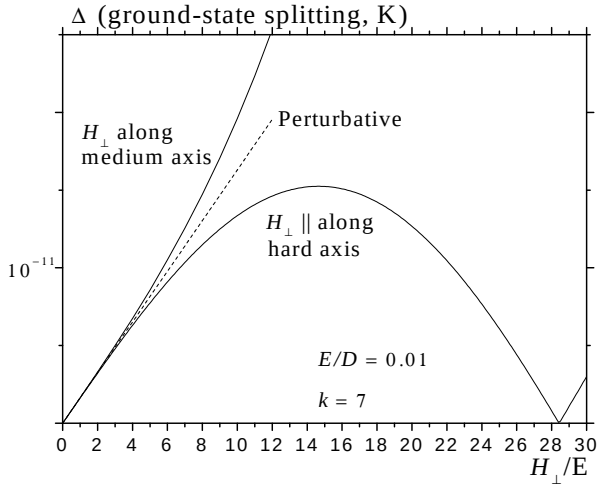

FIG. 5. Exact and perturbative results for the transverse-field dependence of the splitting of the metastable ground-state at the $k = 7$ tunneling resonance.

type and configuration of dislocations, with E and $H_\perp$ being of the same order of magnitude. To obtain tunnel splittings perturbatively in such a model, one has to sum up the products of matrix elements of perturbations and corresponding energy denominators, each product representing a chain connecting the states m and m'.[35] In general, this algorithm is very cumbersome and has no advantages with respect to direct numerical diagonalization of the spin Hamiltonian.

Fortunately, as will become apparent below, for $H_\perp \sim E \ll D$ the effect of the transverse field on tunneling is much weaker than that of the transverse anisotropy. Thus, for the even resonances one can neglect the field contribution to the splittings, whereas for the odd resonances the field should be taken into account in the first order only. In the latter case, the main source of the splitting is the transverse anisotropy taken in a high order of a perturbation theory needed to build a chain of matrix elements that changes the spin projection by $m' - m - 1$. For odd resonances the transverse field makes the missing single perturbation step along that chain, needed to change the spin projection by one. The corresponding matrix element $\langle m_1|H_x S_x|m_1+1\rangle$ can be inserted at any place in the chain, $m_1 = m, m+1, \ldots, m'-1$. Quite fortunately, the corresponding sum can be calculated exactly:

$$\frac{1}{\pi}\sum_{p=0}^{r}\frac{\Gamma(r-p+1/2)\Gamma(p+1/2)}{\Gamma(r-p+1)\Gamma(p+1)} = 1 \qquad (31)$$

and the resulting splittings for odd resonances acquires the elegant form:

$$\Delta_{mm'} = \frac{H_x}{[(m'-m-2)!!]^2} \times\sqrt{\frac{(S+m')!(S-m)!}{(S-m')!(S+m)!}}\left(\frac{|E|}{2D}\right)^{(m'-m-1)/2}. \qquad (32)$$

Note that this perturbative result does not depend on the sign of E, that is, the splitting is the same for the transverse field directed along the medium or hard axes. The difference between these two cases appears in higher orders in the transverse field, see Fig. 5. For the transverse field along the hard axis, there is a destructive interference of the contributions of the transverse field and the transverse anisotropy[54] that cause splittings to vanish at[55,56]

$$H_x = k_x\sqrt{2E(D+E)}. \qquad (33)$$

For the integer spin S the number k_x satisfying the condition $|k_x| + |k| \le 2S+1$ is odd, where k is the tunneling resonance number of Eq. (1). For even resonances k splittings vanish at $k_x = 0, \pm 2, \ldots$, whereas for odd resonances the splittings vanish at $k_x = \pm 1, \pm 3, \ldots$ It is clear from Eq. (33) and from Fig. 5 that the linear dependence of the splitting on the transverse field, as given by Eq. (32), is valid for $H_\perp \ll \sqrt{2ED}$, which is satisfied in our case $H_\perp \sim E \ll D$.

The condition on the transverse field obtained above also follows from simple perturbative arguments. For the matrix element of the perturbation $V_{m_1,m_1+2} = \langle m_1|\hat{V}|m_1+2\rangle$ one has $V_{m_1,m_1+2} \sim E$ if the perturbation is due to the transverse anisotropy, and $V_{m_1,m_1+2} \sim H_\perp^2/D$ if it is due to the transverse field. Thus the effects of both types of perturbation are comparable if $H_\perp \sim \sqrt{ED}$.

Let us compare now the strengths of even and odd tunneling resonances. For an odd resonance the ratio of $\Delta_{mm'}$ to the geometrical mean value of the splittings of adjacent even resonances has the form

$$\frac{\Delta_{mm'}}{\sqrt{\Delta_{m,m'+1}\Delta_{m,m'-1}}} = F(S,m,m')\frac{H_x}{\sqrt{2ED}}, \qquad (34)$$

where

$$F(S,m,m') = \frac{(m'-m-1)!!(m'-m-3)!!}{[(m'-m-2)!!]^2} \times\left[\frac{(S+m')(S-m'+1)}{(S-m')(S+m'+1)}\right]^{1/4}. \qquad (35)$$

The function $F(S,m,m')$ is of order unity. It approaches $\pi/2$ in the quasiclassical case of large S, m, and m'. Thus the odd resonances are weaker than the even ones by the factor of order $H_x/\sqrt{DE}$. This effect is not dramatic since odd and even resonances only differ by a prefactor in front of high power of the small ratio E/D, see Eqs. (30) and (32).

It should be stressed that for numerical calculation of tunnel splittings the *exact* resonance condition[55,56]

$$H_z = k\sqrt{D^2 - E^2}, \qquad k = 0, \pm 1, \pm 2, \ldots \qquad (36)$$

should be used instead of Eq. (1). Although for $E \ll D$ the corrections to the resonance fields H_z due to the transverse anisotropy are small, the detuning of levels arising from the use of the approximate resonance condition of Eq. (1) is much larger than the level splitting. If the exact Eq. (36) was not known (which may well be

the case for more complicated spin models), the numerical finding of level splittings would require sweeping of H_z which is a time-costly procedure.

One of the results of this section is that $S \gg 1$ the slowly decaying perturbations of the spin Hamiltonian due to dislocations, Eq. (7), generate tunnel splittings which change by many orders of magnitude on the distance from the dislocation. Consequently, the behavior of Mn_{12} crystals at low temperatures must be similar to that of disordered systems with widely distributed parameters. The natural scale to discuss physical properties of such systems is logarithmic, which makes the results practically insensitive to any prefactors of order unity, such as the functions $g(\varphi)$ in Eq. (7) encapsulating differences between different types of linear dislocations. For this reason, we will use only one type of dislocations for illustrations, the edge dislocations along the y-axis. Before studying spin-tunneling rates due to dislocations in real Mn_{12} crystals, one should work out one fundamental characteristic of these crystals: the spatial distribution of transverse anisotropies. This will be done in the next section.

IV. DISTRIBUTION OF TRANSVERSE ANISOTROPIES DUE TO DISLOCATIONS

In a crystal with dislocations, the deformation tensor at any given point is a sum of contributions due to many different dislocations. The superposition principle for deformations follows from the linearity of the equations of the theory of elasticity[51] and it holds everywhere outside dislocation cores, i.e., for the distances from the dislocation axes $r \gtrsim 1$. Statistical properties of deformations and thus of the spin tunneling rates in a Mn_{12} crystal depend on the spatial distribution of dislocations which is poorly known. In this section we present analytical solution of the problem of distribution of transverse anisotropies, assuming that dislocations are distributed at random. Note that alternatively, one can consider a regular array of dislocations with alternating directions of the Burgers vector, to achieve a balance of contractions and dilations throughout the crystal. Such a dislocation array should be randomized to some extent to make it more realistic, as was done in Ref. 41.

For the random-dislocation model, one should, in principle, consider different types of dislocations and compute an average over all crystal sites. For simplicity, we will take into account only one type of randomly distributed dislocations with collinear axes: the edge dislocations along the Y-axis, see Sec. IIE, and consider one representative site in the middle of the crystal, $\mathbf{r} = 0$. The distribution function for the transverse anisotropy can be defined as

$$f_{\tilde{E}} = \left\langle \delta\left(\tilde{E} - \sum_{i=1}^{N} \tilde{E}(\mathbf{r}_i)\right)\right\rangle, \qquad \tilde{E} \equiv \frac{E}{2D}, \tag{37}$$

where $N \gg 1$ is the number of dislocations in the crystal and the averaging is carried out over their positions $\mathbf{r}_i$ in the plane perpendicular to the dislocation axis within a circular region of radius R. One can define

$$c = \frac{N}{\pi R^2} = \frac{1}{\pi R_c^2}, \tag{38}$$

where c is the concentration of dislocations and R_c is the characteristic distance between dislocations.

Let us at first analyze the large-$|\tilde{E}|$ asymptotes of $f_{\tilde{E}}$ due to the regions with large deformations of both signs close to one of dislocations. In that case one can neglect the influence of all other dislocations and consider the one-dislocation model

$$f_{\tilde{E}} = \frac{1}{\pi R_c^2}\int_0^{2\pi} d\varphi \int_0^{R_c} r dr \delta\left(\tilde{E} - \frac{g(\varphi)}{r}\right). \tag{39}$$

Integration yields

$$f_{\tilde{E}} = \frac{\tilde{E}_c^2}{|\tilde{E}|^3}, \qquad |\tilde{E}| \gtrsim \tilde{E}_c \equiv \frac{\sqrt{\langle g(\varphi)^2\rangle}}{R_c}, \tag{40}$$

where E_c is the characteristic transverse anisotropy at the distance R_c. This formula becomes invalid for $\tilde{E} \lesssim \tilde{E}_c$, where the lines of constant $\tilde{E}$ in Eq. (39) cross the boundary of the region under consideration, $r = R_c$. In fact, for $\tilde{E} \lesssim \tilde{E}_c$ the very Eq. (39) becomes invalid and one has to take into account other dislocations. Eq. (40) suggests that one should introduce the distribution function for a reduced transverse anisotropy α

$$f_\alpha \equiv \tilde{E}_c f_{\tilde{E}}, \qquad \alpha \equiv \tilde{E}/\tilde{E}_c, \tag{41}$$

which has the asymptote

$$f_\alpha = \frac{1}{|\alpha|^3}, \qquad \alpha \gtrsim 1. \tag{42}$$

In the general case, with the help of the identity $2\pi\delta(x) = \int_{-\infty}^{\infty} d\omega e^{i\omega x}$, the averaging over the coordinates of different dislocations in Eq. (37) can be factorized,

$$f_{\tilde{E}} = \int_{-\infty}^{\infty} \frac{d\omega}{2\pi} e^{i\omega\tilde{E}} f(\omega)^N, \tag{43}$$

where

$$f(\omega) \equiv \frac{1}{\pi R^2}\int_0^{2\pi} d\varphi \int_0^{R} r dr \exp\left(-\frac{i\omega g(\varphi)}{r}\right). \tag{44}$$

As we shall see, in Eqs. (43) and (44), $\omega \sim R_c \ll R$ for $N \gg 1$, thus the argument of the exponential in Eq. (44) is small and $f(\omega)$ is close to unity. Then the exponential can be expanded and integrated, with a log accuracy, in the interval $|\omega| \lesssim r < R$. Given that $\langle g(\varphi)\rangle = 0$, the result has the form

$$f(\omega) \cong 1 - \frac{\omega^2\langle g(\varphi)^2\rangle}{R^2}\ln\frac{c_0 R}{|\omega|\sqrt{\langle g(\varphi)^2\rangle}}, \tag{45}$$

where c_0 is a constant of order unity. Now with the use of Eqs. (38) and (40) one can write

$$f(\omega)^N \cong \exp\left[-(\omega\tilde{E}_c)^2 \ln\frac{c_0\sqrt{N}}{|\omega|\tilde{E}_c}\right]. \qquad (46)$$

At this point one may forget about the initial assumption on the circular form of the spatial region. The shape of the crystal only affects the value of the constant c_0 under the logarithm. Eq. (46) confirms the assumption $\omega \sim 1/\tilde{E}_c \sim R_c$ made above. Now we are prepared to write down the final result which is convenient to formulate in terms of the function f_α defined by Eq. (41)

$$f_\alpha \cong \frac{1}{\pi}\int_0^\Lambda du\cos(\alpha u)\exp\left(-u^2\ln\frac{c_0\sqrt{N}}{u}\right). \qquad (47)$$

Here the cutoff Λ satisfies $1 \ll \Lambda \ll \sqrt{N}$; one cannot integrate up to ∞ since the form if the integrand is only valid for $u \ll \sqrt{N}$. Clearly, for large enough crystals with $N \gg 1$ the result does not depend on Λ. We remind that for the edge dislocations along the Y-axis, the distribution of transverse anisotropies is an even function. This distribution is shown for $\tilde{E} > 0$ in Fig. 6.

Integrating Eq. (47) by parts three times, one can recover the asymptote of f_α at $|\alpha| \gg 1$ which is given by Eq. (42). This power-law asymptote is a consequence of the logarithmic singularity of the integrand in Eq. (47) at $u \to 0$ and it leads to the divergence of the second moment of f_α. On the other hand, for large N the distribution function may be well approximated by Gaussian for not too large α. Indeed, for large N the logarithm in Eq. (47) is weakly dependent on u and can be replaced by a constant. The best value of this constant corresponds to u for which the argument of the exponential equals one. This requires solving a transcendental equation that can be done in a perturbative way. With a good accuracy one can use

$$\ln\frac{c_0\sqrt{N}}{u} \Rightarrow L = \ln\left[c_0\sqrt{N\ln(c_0\sqrt{N})}\right] \qquad (48)$$

which results in the aproximation

$$f_\alpha \cong \frac{1}{2\sqrt{\pi L}}\exp\left(-\frac{\alpha^2}{4L}\right) \qquad (49)$$

which is also shown in Fig. 6.

As the number N of dislocations in the crystal increases, the function f_α of Eq. (47) becomes closer and closer to the Gaussian, whereas the power-law asymptote given by Eq. (42) becomes shifted to the region of very large α where it is hardly visible. This effect is due to the accumulation of small contributions from dislocations situated at large distances from the observation point (of order of the linear dimension of the crystal). Such small contributions from distant dislocations, which lead to the Gaussian distribution f_α, win over contributions from close dislocations responsible for Eq. (42). One can estimate the characteristic value α_1 of the transverse anisotropy at which the distribution function changes its behavior by equating the Gaussian approximation for f_α given by Eq. (49) to its asymptote of Eq. (42). This yields

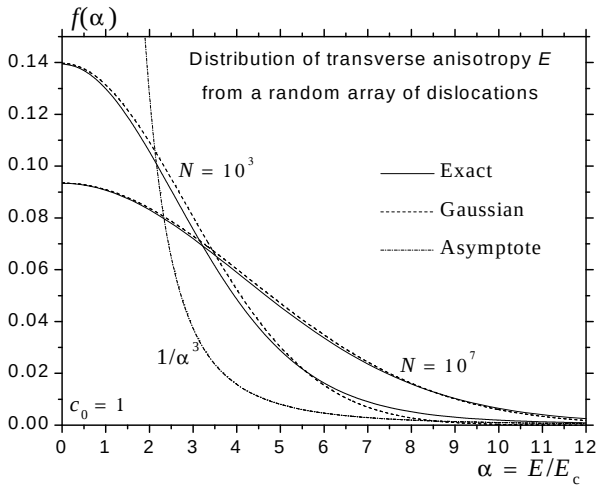

FIG. 6. Distribution of the transverse anisotropy due to a random array of edge dislocations along the Y-axis

$$\alpha_1 \cong \sqrt{4L\ln(4L/\sqrt{\pi})}. \qquad (50)$$

Transverse anisotropies $\tilde{E}$ [see Eqs. (37) and (41)] corresponding to $\alpha > \alpha_1$ are due to a single dislocation in the vicinity of the observation point, whereas $\alpha < \alpha_1$ are collective contributions of many distant dislocations. The characteristic distance r_1 from the dislocation core is defined by $\tilde{E}_1 \equiv \alpha_1\tilde{E}_c = \sqrt{\langle g(\varphi)^2\rangle}/r_1$ and reads

$$r_1 = \frac{R_c}{\alpha_1} = \frac{1}{\sqrt{4\pi cL\ln(4L/\sqrt{\pi})}}. \qquad (51)$$

One can see that in a macroscopic crystal the contribution of a particular dislocation dominates within a distance from its core, r_1, that is small compared to the average distance between the dislocations. The fraction of cites in the lattice affected mostly by one close dislocation is

$$n_1 \cong 2\int_{\alpha_1}^\infty \frac{d\alpha}{\alpha^3} = \frac{1}{\alpha_1^2} = \frac{1}{4L\ln(4L/\sqrt{\pi})}. \qquad (52)$$

This fraction is small if the number of dislocations N in the crystal is large. Molecules belonging to this group may be interpreted as the minor species. One should note that the value of n_1 above is, in fact, only the upper bound on n_1. The asymptote $f_\alpha \cong 1/\alpha^3$ is applicable for $\alpha \gg \alpha_1$ (say, for $\alpha \gtrsim 3\alpha_1$) rather than for $\alpha \gtrsim \alpha_1$. If one replaces α_1 by $3\alpha_1$ in Eq. (52), the value of n_1 will decrease by one order of magnitude.

The Gaussian approximation for the function $f_{\tilde{E}}$ with the help of Eq. (41) can be written in the form

$$f_{\tilde{E}} \cong \frac{1}{2\tilde{E}_{\tilde{c}}\sqrt{\pi}}\exp\left(-\frac{\tilde{E}^2}{(2\tilde{E}_{\tilde{c}})^2}\right), \qquad (53)$$

where

$$\tilde{E}_{\tilde{c}} \equiv \tilde{E}_c\sqrt{L} = \sqrt{\pi\langle g(\varphi)^2\rangle\tilde{c}}, \qquad \tilde{c} \equiv cL. \qquad (54)$$

That is, the accumulation of contributions from distant dislocations leads to the effective logarithmic renormalization of the concentration of dislocations c with L defined by Eq. (48). For edge dislocations along the Y-axis,

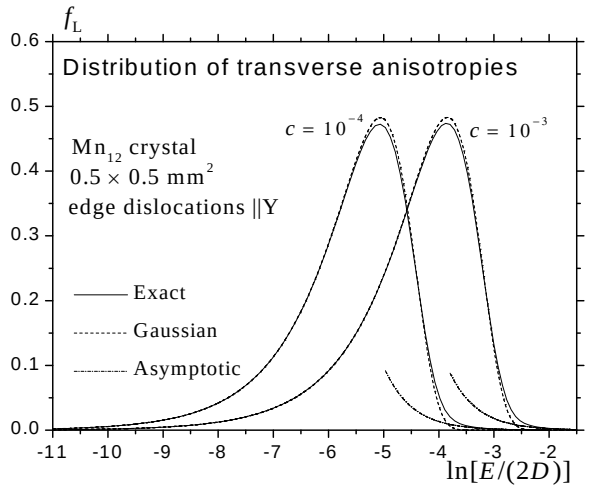

FIG. 7. Distribution of the logarithm of transverse anisotropy due to random array of edge dislocations along the Y-axis

the quantity $\sqrt{\langle g(\varphi)^2\rangle}$ according to Eqs. (7), (28), and (23) is given by

$$\sqrt{\langle g(\varphi)^2\rangle} = \frac{g_1\sqrt{5-12\sigma+8\sigma^2}}{8\pi(1-\sigma)}, \tag{55}$$

where σ is the Poisson elastic coefficient. For for $g_1 = 1$ and $\sigma = 0.25$ one has $\sqrt{\langle g(\varphi)^2\rangle} \approx 0.084$.

The experimentally studied Mn_{12} crystals are rather large, about 0.5×0.5 mm^2, which corresponds to the cross-section of about 10^{11} lattice cells. Even for the concentration of dislocations as small as $c = 10^{-4}$ per cell, the number of dislocation in the crystal is about $N \approx 10^7$. For $c_0 = 1$ this gives $L = 9.1$, i.e., the effective concentration of dislocations increases by an order of magnitude, $\tilde{c} = 0.91 \times 10^{-3}$. The corresponding value of $\tilde{E}_{\tilde{c}}$ that follows from Eqs. (54) and (55) is $\tilde{E}_{\tilde{c}} = 0.449 \times 10^{-2}$. For $c = 10^{-3}$ one obtains $L = 10.3$, thus $\tilde{E}_{\tilde{c}} = 1.51 \times 10^{-2}$. If one takes $L \approx 10$, then Eq. (52) yields $n_1 \approx 1/125$. That is, less than 1% of all Mn_{12} molecules in the crystal belong to the fast relaxing group in the vicinity of a single dislocation. In fact, the value of n_1 should be much smaller, see comment after Eq. (52). The renormalization of the concentration of dislocations and the Gaussian distribution of transverse anisotropies for large crystals are clearly seen in Fig. 6: The distribution becomes broader in the α-scale due to the increase L with N, Eq. (48).

Having determined the distribution of transverse anisotropies created by dislocations in a Mn_{12} crystal, we can calculate the distribution of tunnel splittings for different level pairs and different resonances. This will be done in the next section, where we will use the distribution of the logarithm of the transverse anisotropy

$$f_L(x) = 2e^x f_{\tilde{E}}(e^x), \qquad x \equiv \ln\tilde{E}. \tag{56}$$

If the Gaussian approximation for $f_{\tilde{E}}$, Eq. (53), is adopted, then f_L has the form

$$f_L(x) \cong \frac{1}{\tilde{E}_{\tilde{c}}\sqrt{\pi}} \exp\left(x - \frac{e^{2x}}{(2\tilde{E}_{\tilde{c}})^2}\right). \tag{57}$$

This function is plotted in Fig. 7 for $c = 10^{-3}$ ($\tilde{E}_{\tilde{c}} \approx 1.51 \times 10^{-2}$) and $c = 10^{-4}$ ($\tilde{E}_{\tilde{c}} \approx 0.449 \times 10^{-2}$).

V. DISTRIBUTION OF TUNNEL SPLITTINGS

Distribution of transverse anisotropies due to dislocations, which was obtained in the previous section, determines the distribution of the tunnel splittings which for the even-k resonances are given by Eq. (30). It is convenient to rewrite Eq. (30) in terms of the resonance number k and the level number $n = 0, 1, \ldots$ in the metastable well of negative spin projections

$$m = n - S, \qquad m' = S - n - k. \tag{58}$$

Thus Eq. (30) becomes

$$\Delta_{nk} = g_{nk}\tilde{E}^{\xi_{nk}} \qquad (k \text{ even}), \tag{59}$$

where $\tilde{E} \equiv E/(2D)$, $\xi_{nk} \equiv S - n - k/2$, and

$$g_{nk} \equiv \frac{2D}{[(2S-2n-k-2)!!]^2}\sqrt{\frac{(2S-n-k)!(2S-n)!}{(n+k)!n!}}. \tag{60}$$

With the help of Eq. (59) one can write down the distribution of the square of tunnel splittings for any resonance in terms of the previously defined $f_{\tilde{E}}$

$$f_{\Delta^2_{nk}}(\Delta^2) = \frac{1}{\xi_{nk}g^2_{nk}}\left[\frac{\Delta^2}{g^2_{nk}}\right]^{\frac{1}{2\xi_{nk}}-1} f_{\tilde{E}}\left[\left(\frac{\Delta^2}{g^2_{nk}}\right)^{\frac{1}{2\xi_{nk}}}\right]. \tag{61}$$

Because ξ_{nk} is a large number, especially for resonances with small n and k, tunnel splittings in a Mn_{12} crystal spead over many orders of magnitude, from rather large values near dislocation cores to very small values far from dislocations. It is thus more convenient to consider the distribution of the decimal logarithm of tunnel splittings, $y \equiv \log_{10}\Delta$. With the help of Eq. (59) it can be written as

$$f_{\log_{10}\Delta}(y) = \frac{\ln 10}{\xi_{nk}} f_L\left(\frac{y\ln 10 - \ln g_{nk}}{\xi_{nk}}\right). \tag{62}$$

Here $f_L(x)$ is the distribution function of $x = \ln\tilde{E}$ defined by Eq. (56). Distribution of the ground-state ($n = 0$) tunnel splittings for different resonance numbers k is shown in Fig. 8 for a Mn_{12} crystal of size 0.5×0.5 mm^2 with concentration of dislocations $c = 10^{-3}$. One can see that the distribution is shifted to the left and becomes broader for smaller k.

For odd tunneling resonances, the splitting, according to Eq. (32), depends on both the transverse anisotropy and the transverse field which are generated by dislocations. Since the functions $g(\varphi)$ and $g_H(\varphi)$ in Eq. (7) are different, one cannot, strictly speaking, express the distribution of splittings via that of the transverse anisotropy alone. Fortunately, transverse field is only a prefactor in front of a small term in Eq. (32). This allows one to

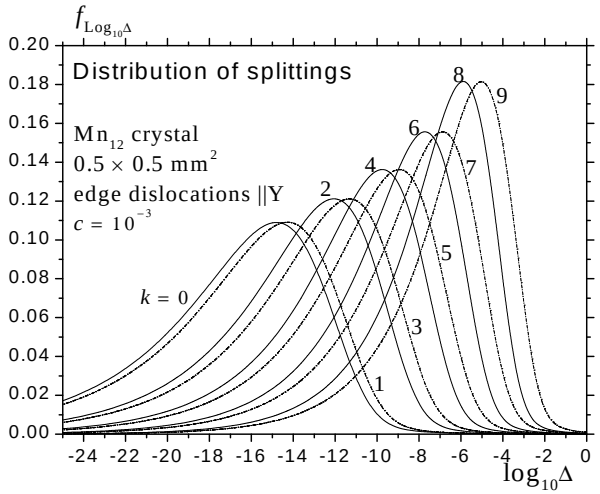

FIG. 8. Distribution of the logarithm of the ground-state ($n = 0$) tunnel splittings due to a random array of edge dislocations along the Y-axis

express $H_\perp$ via E with the help of Eq. (7) and use the resonance condition $H_z = kD$ to obtain

$$\frac{H_x}{2D} = \frac{k\tilde{E}}{2}\frac{g_H(\varphi)}{g(\varphi)} \Rightarrow \frac{k\tilde{E}}{2}c_{\mathrm{odd}}, \tag{63}$$

with the ratio of angular functions approximated by a constant $c_{\mathrm{odd}} \sim 1$. In this approximation, the level splittings at odd k are functions of the transverse anisotropy alone, so that one can rewrite Eq. (32) as

$$\Delta_{nk} = g'_{nk}\tilde{E}^{\xi'_{nk}} \qquad (k \ \text{odd}), \tag{64}$$

where

$$g'_{nk} \equiv \frac{ck}{2}g_{nk}, \qquad \xi'_{nk} = \xi_{nk} + \frac{1}{2} = S - n - \frac{k-1}{2} \tag{65}$$

[cf. Eqs. (59) and (60)]. For the distribution of the decimal logarithm of splittings at odd resonances one obtains the formula analogous to Eq. (62) where the constant c enters under the logarithm. Note that the power ξ'_{nk} for an odd resonance is the same as the power ξ_{nk} for the preceding even resonance, thus the splitting distribution functions for these two resonances differ, according to Eq. (62), only by a shift. This is clearly seen on Fig. 8 where we have plotted the odd-resonance curves for $c_{\mathrm{odd}} = 1$.

If the distribution of the level splittings for different k is simulated, as was done in Ref. 41, or is measured, the theory developed above could be tested by re-plotting the data in terms of the scaling variable[41]

$$x = \frac{1}{\xi_{nk}} \ln \frac{\Delta_{nk}}{g_{nk}}. \tag{66}$$

Since $x = \ln \tilde{E}$, it does not depend on the numbers n and k, thus all the curves should scale. For odd resonances, one should use ξ'_{nk} and g'_{nk} of Eq. (65), where c can be considered as an adjustable parameter.

VI. INCOHERENT LANDAU-ZENER PROCESSES

A very convenient method to experimentally study spin tunneling consists of sweeping the longitudinal field, thus making a pair of levels on different sides of the barrier, ε_n and $\varepsilon_{n'}$, to go through a resonance.[9,57] For a purely quantum-mechanical system, the probability of the system to stay in the same well (i.e., to go from one *exact* energy branch to the other) is given by[36,37,38]

$$P = \exp\left(-\frac{\pi\Delta_n^2}{2v_n}\right), \tag{67}$$

where Δ_n is the level splitting and $v_n \equiv |d(\varepsilon_{n'} - \varepsilon_n)/dt|$ is the speed of the level detuning *unperturbed* by the tunneling interaction, i.e., the energy sweep rate. Landau[36] has obtained this formula in the special case of a large argument of the exponential (low sweep rates), whereas Zener[37] obtained it for all sweep rates, however with a wrong additional factor 2π in the exponential. Recent Ref. 38 reproduces Zener's results without the wrong factor 2π [Eq. (11) of Ref. 38 is equivalent to Eq. (67)]. We will call this process the *coherent* Landau-Zener process.

For systems interacting with the environment, the situation changes if the linewidth Γ_n of the level is greater than the level splitting Δ_n. This, in fact, happens in most cases, since Δ_n for spin systems is a high power of a small perturbation, while Γ_n is due to transitions between the levels in the same well which appear in much lower order of the perturbation theory on spin-phonon (or other) interactions. The only exception is the tunneling resonance between the ground-state levels in the two wells at low temperatures because the phonon processes contributing to their linewidths die out exponentially at $T \to 0$. If at least one of the resonant levels is not the lowest level in the well, it has a considerable linewidth down to $T = 0$ due to the transitions onto lower levels in the same well, accompanied by the emission of phonons. In this case $\Gamma_n \gg \Delta_n$ and tunneling becomes mediated by the environment, i.e., incoherent.

Incoherent spin tunneling should be described in terms of the density matrix equation rather than in terms of the Schrödinger equation.[13] Since at low temperatures the escape process (via tunneling or via thermal activation) is much slower than the equilibration within the wells, one can eliminate the non-diagonal elements of the density-matrix equation and obtain the system of equations for the level populations that describes tunneling, Eq. (4.12) of Ref. 13. In sweeping-field experiments on Mn_{12} in the kelvin or subkelvin range, the backflow of particles from the stable to the metastable well is exponentially small and can be safely neglected for all resonances with $k \neq 0$, since the corresponding activation energy is about $2SD \simeq 13$K. Thus there is only one-way escape from the metastable well described by the equation[13]

$$\dot{N}_0 = -\sum_{n=0}^{n_{\mathrm{top}}} N_n \frac{\Delta_{nk}^2}{2} \frac{\Gamma_{nn'}}{(\varepsilon_{n'} - \varepsilon_n)^2 + \Gamma_{nn'}^2}, \tag{68}$$

where $\Gamma_{nn'} \equiv \Gamma_n + \Gamma_{n'}$, the numbering of levels begins from the metastable ground state, $n = m + S$, and n_{top}

corresponds to the top of the barrier. The tunnel splitting Δ_{nk} depends on both the level number n in the metastable well and the number of the resonance k of Eq. (1). They are given by Eqs. (30) and (32) with $m = n-S$ and $m' = S-n-k$. In the kelvin and subkelvin temperature range almost all Mn_{12} molecules in the metastable well are in the ground state, whereas the populations of the excited states entering Eq. (68) are exponentially small and are given by the equilibrium formulas

$$N_n = N_0 e^{-\Delta\varepsilon_{nk}/T}, \qquad \Delta\varepsilon_{nk} = \varepsilon_n - \varepsilon_0, \tag{69}$$

where the level energies are taken at the resonant values of the field, $H_z = kD$ ($k \geq 0$)

$$\varepsilon_n = Dn(2S-n-k) - DS(S-k). \tag{70}$$

Now Eq. (68) can be integrated for the field sweeping across the resonance. For the constant energy-sweep rate

$$\varepsilon_{n'} - \varepsilon_n = v_{nk}t + \text{const}, \tag{71}$$

where $v_{nk} = (2s-2n-k)dH_z/dt$, one obtains

$$N_0^{(k,\text{after})} = N_0^{(k,\text{before})} \exp\left[-\sum_{n=0}^{n_{\max}} \frac{\pi\Delta_{nk}^2 e^{-\Delta\varepsilon_{nk}/T}}{2v_{nk}}\right], \tag{72}$$

where $N_0^{(k,\text{before})}$ and $N_0^{(k,\text{after})}$ are the numbers of Mn_{12} molecules in the metastable well before and after crossing the k-resonance.

Eq. (72) describes a superposition of incoherent Landau-Zener tunneling processes which come both directly from the metastable ground state and via excited states. At $T = 0$ the result coincides with that of Eq. (67), although the physics is different. Note that for the incoherent Landau-Zener tunneling between the two lowest-energy states one has to take into account the flow of particles in both directions, which results in the disappearance of the factor 2 in the denominator of Eq. (72).[40] In this situation, however, one should carefully check the applicability condition of the method, $\Gamma_n \gg \Delta_n$, since Γ_n may be very small. Incidentally, for Mn_{12} acetate the tunneling between the ground states is so weak that the $k = 0$ resonance cannot be observed experimentally, unless a strong transverse field is applied.

The field sweeping technique is a very convenient experimental tool since Eq. (72) does not depend on the damping parameters which are difficult to determine with sufficient accuracy. The combination $\Delta_{nk}^2 e^{-\Delta\varepsilon_{nk}/T}$ is familiar from Refs. 13, 20, 21 where it was used to investigate the transition on temperature between thermally activated and tunneling regimes of the escape from the metastable well. To be more precise, let us rewrite Eq. (72) with the help of

$$\begin{aligned} &v_{nk} = \delta\varepsilon_{nk}\tilde{v}, \qquad \tilde{v} \equiv \frac{1}{D}\frac{dH_z}{dt} \\ &\delta\varepsilon_{nk} \equiv \varepsilon_n - \varepsilon_{n-1} = D(2S-2n-k) \end{aligned} \tag{73}$$

where $\delta\varepsilon_{nk}$ is the level spacing in the well. One obtains

$$N_0^{(k,\text{after})} = N_0^{(k,\text{before})} \exp\left[-\sum_{n=0}^{n_{\max}} \frac{\pi f_{nk}(T)}{2\tilde{v}}\right], \tag{74}$$

where

$$f_{nk}(T) \equiv \frac{\Delta_{nk}^2}{\delta\varepsilon_{nk}} e^{-\Delta\varepsilon_{nk}/T}. \tag{75}$$

In fact, this form of f_{nk} is valid when the tunnel splitting is small, $\Delta_{nk} \ll \delta\varepsilon_{nk}$. This is true for energy levels below the top of the barrier. Near the top of the barrier, where $\Delta_{nk} \sim \delta\varepsilon_{nk}$, a more accurate formula is[20]

$$f_{nk}(T) \equiv \frac{\delta\varepsilon_{nk}\Delta_{nk}^2}{(\delta\varepsilon_{nk})^2 + (\pi\Delta_{nk})^2} e^{-\Delta\varepsilon_{nk}/T}. \tag{76}$$

It ensures that $f_{nk} \sim \delta\varepsilon_{nk} e^{-\Delta\varepsilon_{nk}}$ near the top of the barrier for any approximation used for Δ_{nk}.

Since $f(n)$ is a product of the two functions, one of which rapidly increases and the other rapidly decreases as n goes up, there is a narrow group of levels around $n = n^*(T)$ that maximizes $f_{nk}(T)$ and makes the dominant contribution to the Landau-Zener transition. Above the quantum-classical transition temperature T_0, one has $n^*(T) = n_{\text{top}}$, which corresponds to the activated regime with the spin escaping over the top of the barrier. As T is lowered below T_0 the tunneling level goes down, which corresponds to the thermally assisted tunneling or, at even lower temperatures, to the ground-state tunneling. If $n^*(T)$ is continuous, one can speak about the second-order quantum-classical transition. If $n^*(T)$ jumps over several levels at some temperature, the transition is first order. 13, 20, 21 Recently an experimental evidence of the first-order transition in Mn_{12} has been obtained in Refs. 11, 12. (The biaxial model with the magnetic field along the hard axis shows two first-order transitions in some range of parameters.[24,21])

Experimental study of the temperature dependence of the tunneling level $n^*(T)$ in Mn_{12} is possible due to the small quartic-anisotropy term $-AS_z^4$ in the spin Hamiltonian, which makes the resonance fields H_z dependent of the quantum number n. Tunneling resonance between higher pairs of levels takes place at slightly lower value of H_z than the resonance between lower pairs of levels, that is, the k-resonance has a fine structure. Measuring temperature dependence of the resonance field H_z for a given k gives the information on the level n that dominates tunneling at a given temperature.[11,12] Eq. (72) remains correct if the resonances for different n take place at different values of the field H_z, provided that the field is being swept through all these resonances. If different n-resonances are well separated from each other, which is the case for Mn_{12}, then for each n-resonance one obtains

$$N_0^{(n,k,\text{after})} = N_0^{(n,k,\text{before})} \exp\left[-\frac{\pi\Delta_{nk}^2 e^{-\Delta\varepsilon_{nk}/T}}{2v_{nk}}\right] \tag{77}$$

[cf. Eq. (72)].

VII. LANDAU-ZENER RELAXATION IN SYSTEMS WITH DISTRIBUTED PARAMETERS

As follows from the above, in Mn_{12} crystals with dislocations the tunnel splittings Δ_{nk} differ from one Mn_{12} molecule to another. Thus the fraction of Mn_{12} molecules that stay in the metastable well after crossing the n-resonance,

$$R_{nk} \equiv \frac{N_0^{(n,k,\mathrm{after})}}{N_0^{(n,k,\mathrm{before})}} \tag{78}$$

is an average that must be computed with the help of the distribution function of Eq. (61)

$$R_{nk}(\tilde{v}) = \int_0^\infty d\Delta^2 f_{\Delta_{nk}^2}(\Delta^2) \exp\left[-\frac{\pi f_{nk}(\Delta,T)}{2\tilde{v}}\right], \tag{79}$$

where f_{nk} is given by Eq. (76). As was argued after Eq. (61), the distribution of splittings is so broad that the natural scale to represent it is logarithmic. On the logarithmic scale, one can replace the exponential by a step function, $e^x \Rightarrow \theta(1-x)$. This gives

$$R_{nk}(\tilde{v}) \cong \int_0^{\Delta_{nk,v}^2} d\Delta^2 f_{\Delta_{nk}^2}(\Delta^2), \tag{80}$$

where $\Delta_{nk,v}^2$ is the solution of the equation

$$\pi f_{\Delta_{nk}^2}(\Delta^2)/(2\tilde{v}) = 1 \tag{81}$$

for Δ^2. With the help of Eq. (76) we get

$$\Delta_{nk,v}^2 = \left(\frac{\delta\varepsilon_{nk}}{\pi}\right)^2 \frac{\tilde{v}}{\tilde{v}_{nk}^{\max} - \tilde{v}}, \qquad \tilde{v} < \tilde{v}_{nk}^{\max}, \tag{82}$$

and $\Delta_{nk,v}^2 = \infty$ for $\tilde{v} \geq \tilde{v}_{\max}$, where

$$\tilde{v}_{nk}^{\max} \equiv \frac{\delta\varepsilon_{nk}}{2\pi} e^{-\Delta\varepsilon_{nk}/T}. \tag{83}$$

The physical meaning of Eq. (79) is the following. Since the tunnel splitting Δ is a high power of the transverse anisotropy E, there is very few Mn_{12} molecules with $\Delta_{nk} \sim \Delta_{nk,v}$, whereas most of the molecules have $\Delta_{nk} \ll \Delta_{nk,v}$ or $\Delta_{nk} \gg \Delta_{nk,v}$. Eq. (79) simply ignores the small group of Mn_{12} molecules with $\Delta_{nk} \sim \Delta_{nk,v}$. The quantity $\tilde{v}_{nk}^{\max}$ is the maximal sweep rate $\tilde{v}$ for which the Landau-Zener transition for the given n, k, and T is possible. For $\tilde{v} \geq \tilde{v}_{nk}^{\max}$ one cannot find Mn_{12} molecules that relax fast enough to satisfy Eq. (79), since the transition probability has an upper bound on Δ which is described by Eq. (76). Eq. (80) can be rewritten in terms of the distribution function for the logarithm of the transverse anisotropy, Eq. (56). It then becomes

$$R_{nk} \cong \int_{-\infty}^{x_{nk,v}} dx f_L(x), \tag{84}$$

where $x_{nk,v} = \ln \tilde{E}_{nk,v}$ and $\tilde{E}_{nk,v}$ is the transverse anisotropy needed to create the value of splitting $\Delta_{nk,v}$. With the help of Eqs. (82) and (59) we get

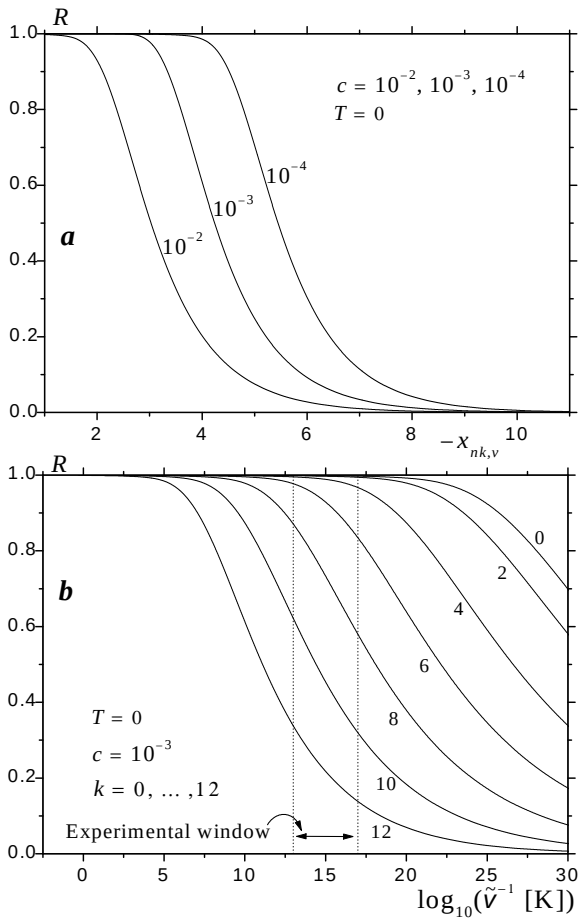

FIG. 9. a – Probability of remaining in the metastable well R as a function of the scaling argument $-x_{nk,v}$ [see Eq. (85)] at $T = 0$; b – relaxation curves R as functions of the sweep rate for different resonances k.

$$x_{nk,v} = \frac{1}{\xi_{nk}} \ln\left[\frac{\delta\varepsilon_{nk}}{\pi g_{nk}} \sqrt{\frac{\tilde{v}}{\tilde{v}_{\max} - \tilde{v}}}\right] \tag{85}$$

One can see from Eq. (84) that the relaxation curves R_{nk} for the n,k-resonance, when represented in terms of $x_{nk,v}$, depend only on the distribution of transverse anisotropies in the crystal and scale onto the same curve. If the Gaussian approximation for the anisotropy-distribution function is used, see Eqs. (53) and (57), $R_{nk}(x_{nk,v})$ can be expressed via the error function. The relaxation curves at $T = 0$ are shown in Fig. 9 both in the scaling form, as functions of $-x_v$, and in the natural form, as a function of $\log_{10}(1/\tilde{v})$ for even k. For odd k the relaxation curves (not shown) differ by a shift from the ajacent even-k curves, see Fig. 8. The curves in Fig. 9b have been plotted with the help of the simplified Eq. (80). The deviation from the exact Eq. (79) is rather small and it can be further reduced if one uses the improved formula

$$R_{nk} \cong \int_{-\infty}^{x_{nk,v}} dx f_L(x) - \frac{C}{2\xi_{nk,v}} f_L(x_{nk,v}), \tag{86}$$

where $C = 0.577216$ is the Euler constant. Note that the $1/\xi_{nk}$ correction above has a non-scaling form. This

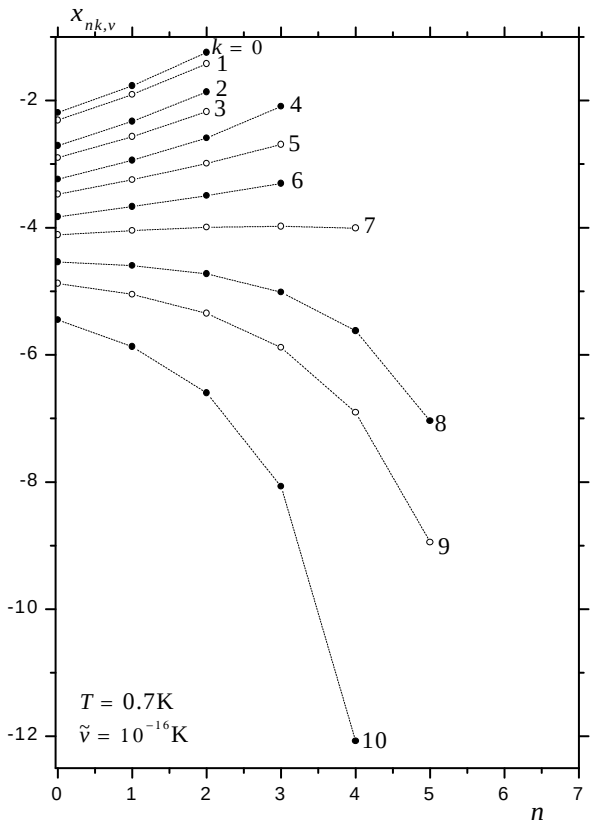

FIG. 10. Dependence of $x_{nk,v} = \ln \tilde{E}_{kn,v}$ [see Eq. (85)] on the excited level n at different k for $T = 0.7$K and $\tilde{v} = 10^{-16}$.

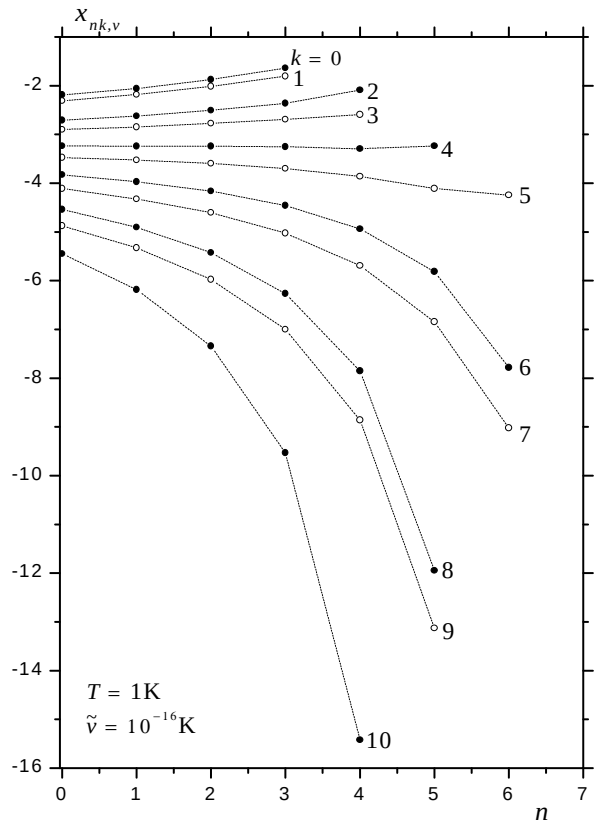

FIG. 11. The same for $T = 1$K.

correction is equivalent to a small shift of the relaxation curves in Fig. 9 to the left:

$$x_{nk} \Rightarrow \tilde{x}_{nk} = x_{nk} - C/(2\xi_{nk}). \tag{87}$$

As we have seen in Sec. V, distributions of tunnel splittings for any n and k are functions of the distribution of transverse anisotropies, which is the basic characteristic of the Mn_{12} crystal. Field-sweeping measurements in the subkelvin temperature range, where transitions via excited levels, $n > 0$, are negligible, provide the means of extracting that distribution. For odd k-resonances, one should use Eq. (64) and fit the constant $c_{\rm odd}$.

At higher temperatures, tunneling transitions via excited states $n > 0$ become activated. The resonances with higher n occur at lower values of the longitudinal field H_z because of the small term $-AS_z^4$ in the spin Hamiltonian. In an ideal Mn_{12} crystal, field-sweeping experiments could provide the information on the level $n^*(T)$ which maximizes the function f_{nk} and thus dominates the escape process at temperature T. Here the field sweep should not be too slow, otherwise crossing the resonances with higher n will cause depletion of the metastable well and resonances with lower n will not be seen. In real Mn_{12} crystals with dislocations, the situation changes drastically because of the broad distribution of tunneling rates. The depletion becomes unavoidable because for any $\tilde{v} < \tilde{v}_{nk}^{\max}$ most of Mn_{12} molecules in the crystal belong to one of two groups. Molecules of the first group cross the barrier with a probability close to one, while molecules of the second group stay in the metastable well with a probability close to one. The whole process strongly depends on the history of the sample, in particular, on the direction of the field sweep. If the field is increasing, then at the n,k-th resonance the Mn_{12} molecules which cross the barrier satisfy

$$\Delta_{nk,v} < \Delta_{nk} \qquad \text{but} \qquad \Delta_{n+1,k} < \Delta_{n+1,k,v}, \tag{88}$$

where $\Delta_{nk,v}$ is given by Eq. (82). The molecules with $\Delta_{n+1,k,v} < \Delta_{n+1,k}$ cannot cross the barrier at the nth resonance because they have already left the metastable well at the $(n+1)$-th resonance. The inequalities in Eq. (88) determine the range of the logarithm of the transverse anisotropy $x = \ln \tilde{E}$

$$x_{nk,v} < x < x_{n+1,k,v} \tag{89}$$

for molecules that are going to escape at the nth resonance. The fraction of these molecules, which determines the magnetization step at the resonance, is given by

$$P_{nk,v} = \int_{x_{nk,v}}^{x_{n+1,k,v}} dx f_L(x). \tag{90}$$

If H_z is increasing through a value at which the barrier disappears, all Mn_{12} molecules will escape, $\sum_{nk} P_{nk,v} = 1$. With increasing temperature or lowering the sweep rate, the depletion effects become stronger and stronger, which leads to the disappearance of tunneling resonances at certain n and k. Mathematically it manifests itself in

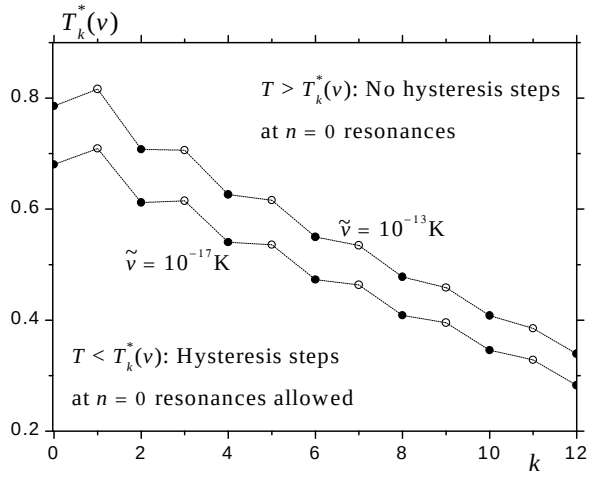

FIG. 12. The values $T_k^*(\tilde{v})$ separating regions with and without hysteresis steps at $n = 0$ resonances.

the disappearance of the x-interval in Eq. (89), which leads to $P_{nk,v} = 0$.

To see which resonances are active and which are not, it is convenient to plot $x_{nk,v}$ of Eq. (85) versus n for different k, Figs. 10 and 11. For $dH_z/dt > 0$, the resonances are crossed in the order from small k to large k and, within a given k-resonance, from the right to the left. If the value of $x_{nk,v}$ decreases, the x-interval in Eq. (89) does exist and the resonance is active. In the opposite case the resonance vanishes. This happens for the resonances with high k in Figs. 10 and 11. Note that the maximal value of n for each k-resonance, $n_{\max}$, is the greatest n satisfying $\tilde{v} < \tilde{v}_{nk}^{\max}$. In the limit $T \to 0$ the maximal velocity $v_{\max}$ of Eq. (83) goes to zero for all $n > 0$. As a result, on lowering T, the branches of $x_{nk,v}$ in Figs. 10 and 11 become shorter and shorter and eventually reduce to the set of $n = 0$ points along the vertical axis. This is in accordance with the obvious fact that at $T = 0$ only transitions from the metastable ground state, $n = 0$, are possible. With increasing temperature, the branches of move down for $n > 0$, and the ground-state resonances disappear one after the other. The same occurs if the sweep rate $\tilde{v}$ decreases. The dependence of $x_{nk,v}$ on $\tilde{v}$, however, is only logarithmic [see Eq. (85)], so that the disappearance of the ground-state resonances at temperatures well below 1K requires unrealistically small values of $\tilde{v}$.

Note that the slope of the branches $x_{nk,v}$ in Figs. 10 and 11 changes for a certain combination of parameters k, T, or $\tilde{v}$ for which the dependence $x_{nk,v}$ on n is nearly flat. One can estimate where it happens from the condition $x_{0k,v} = x_{1k,v}$. For the temperature $T_k^*(\tilde{v})$ corresponding to this transition we get

$$T_k^*(\tilde{v}) \cong \frac{D(2S-1-k)}{\ln Q_v}$$
$$Q_v \equiv \frac{g_{1k}^2 \delta\varepsilon_{0k}}{g_{0k}^2 \delta\varepsilon_{1k}} \left(\frac{\pi g_{0k}^2}{2\tilde{v}\delta\varepsilon_{0k}} \right)^{1/\xi_{0k}}. \qquad (91)$$

This dependence is shown in Fig. 12 for two different sweep rates corresponding to the boundaries of a typical experimental window. In Mn_{12} crystals with dislocations, temperature $T_k^*(\tilde{v})$ plays the role similar to that of temperature T_{00} for an ideal Mn_{12} crystal [cf. Eq. (6.1) of Ref. 13]. The latter is the boundary between the pure ground-state tunneling and the thermally assisted tunneling. It can be obtained by equating $\Delta_{0k}^2/\delta\varepsilon_{0k}$ and $(\Delta_{1k}^2/\delta\varepsilon_{1k})e^{-\Delta\varepsilon_{1k}/T}$. With the help of Eq. (59) one obtains

$$T_{00,k} = \frac{D(2S-1-k)}{\ln Q_E}, \qquad Q_E \equiv \frac{g_{1k}^2 \delta\varepsilon_{0k}}{g_{0k}^2 \delta\varepsilon_{1k}} \frac{1}{\tilde{E}^2}. \qquad (92)$$

In a crystal with dislocations the anisotropy $\tilde{E}$ is distributed and its role is played by the sweep rate $\tilde{v}$ that "chooses" from the distribution of $\tilde{E}$ the matching value of $\tilde{E}$ satisfying Eq. (81) with $n = 0$. Substitution of the solution of that equation, Eq. (85), into Eq. (92), gives Eq. (91).

The temperature $T_{00,k}$ is close to the quantum-classical transition temperature T_0 (see Refs. 13, 14) if the transition is first order. Since for the model with transverse anisotropy the boundary between the first- and second-order transitions is $E_0 = D/3$ (Ref. 16), which corresponds to $\tilde{E}_0 = 1/6$, the values $\tilde{E} \ll 1$ in the main part of the Mn_{12} crystal fall into the range of first-order transition. Accordingly, the change between the two regimes in Figs. 10 and 11 is abrupt: The minimum of $x_{nk,v}$ at $n = 0$ is replaced by the minimum at $n = n_{\max}$, at $T \approx T_k^*(\tilde{v})$. To study second-order transitions, one should use much greater sweep rates $\tilde{v}$ which will shift the curves in Figs. 10 and 11 to higher values of transverse anisotropies $\tilde{E}$. This alone, however, does not guarantee that $P_{nk,v}$ of Eq. (90) is large enough for the effect to be observed. For realistic concentrations of dislocations the values of f_L in that range of $\tilde{E}$ are very small, see Fig. 6.

VIII. RELAXATION IN THE THERMALLY ACTIVATED REGIME

As was commented below Eq. (76), at temperatures above the quantum-classical transition, $T > T_0$ the spins of Mn_{12} molecules escape over the top of the barrier through $n = n_{\text{top}}$, since this value of n maximizes the function f_{nk}. It is interesting to note, however, that Eq. (76) describes Landau-Zener transitions in the field-sweep setup, thus Eqs. (74) and (77) are only valid if it is the resonant tunneling that is dominating the escape. If the spins escape over the top of the barrier, it is no longer important whether the levels are in resonance or not, so that the steps in the dynamic hysteresis curves due to the Landau-Zener transitions should be washed out.

Resonant transitions can still be detected at $T \gtrsim T_0$ due to the reduction of the effective energy barrier in measurements of the time relaxation and of the linear dynamic susceptibility because tunneling at resonance occurs via the level pair for which Δ_{nk} is comparable with the level width $\Gamma_{nn'}$ (Ref. 13). These levels are lower than those at the top of the barrier that satisfy

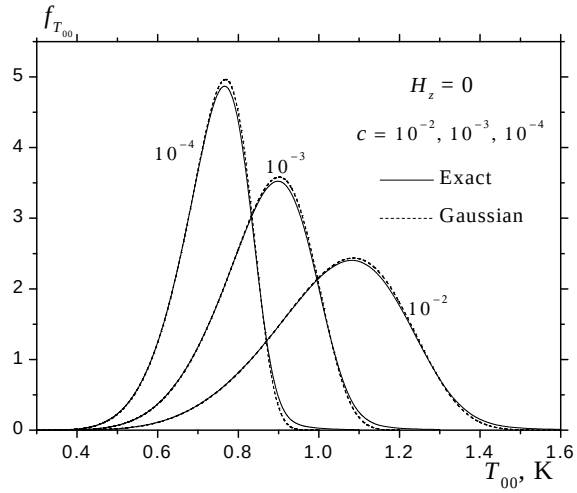

FIG. 13. Distribution of the transition temperatures T_{00} of Eq. (92) in Mn_{12} crystals with dislocations. Dashed lines correspond to the Gaussian approximation of Eq. (57)

.

$\Delta_{nk} \sim \delta\varepsilon_{nk}$. However, in the field-sweep setup the main contribution to the escape rate comes from the levels at the top of the barrier, which makes the escape process non-resonant. A seeming paradox is that resonant tunneling transitions are observed in the dynamic hysteresis experiments in the activation regime.[6] This paradox can be resolved if one takes into account the distribution of T_0 in a non-ideal Mn_{12} crystal. Then some of Mn_{12} molecules have $T_0 < T$, while others have $T_0 > T$, making tunneling resonances weaker but still present as long as there are molecules with $T_0 > T$. Since for realistic concentrations of dislocations the typical values of the transverse anisotropy satisfy $E \ll D$, the quantum-classical transition is first order and a good estimation for T_0 is the temperature T_{00} given by Eq. (92). The distribution of T_{00} can be obtained from the distribution of $\ln \tilde{E}$, see Eqs. (56) and (57). This distribution has an appreciable width, especially for high concentration of dislocations, see Fig. 13. In experiments, quantum steps in the hysteresis have been observed at temperatures as high as 2.8K. This may be either an indication that the fine tuning of the theory (see below) is needed or an indication that Mn_{12} crystals, or even molecules themselves, contain some stronger defects than studied in this paper. Note that for $E = E_0 = D/3$ (which is the boundary between the first- and second-order transition) one has $T_0 = SD/\pi \approx 2$K (Ref. 16).

Since the first-order transition is sharp, there are two groups of Mn_{12} molecules: Molecules of the first group escape via thermal activation over the top of the barrier, while molecules of the second group escape via the ground-state tunneling. Theoretical analysis of this situation is more cumbersome since the basic Eqs. (74) and (77) are valid only for a fraction of Mn_{12} molecules in the crystal. It is thus better to step back to Eq. (68) that yields a greater slope of the dynamic hysteresis curve at resonances and smaller but nonzero slope off resonances. We do not attempt to solve this problem in this article. Instead, we will consider for simplicity the time relaxation off resonance in the activation regime using the classical model, to demonstrate that the relaxation is non-exponential due to dislocations.

For the classical model with transverse anisotropy $E \ll D$, the energy barrier is given by

$$U = U(E) \cong U_0 - \Delta U,$$
$$U_0 = DS^2(1-h_z)^2, \qquad \Delta U = |E|S^2(1-h_z^2), \qquad (93)$$

Ideal crystal

where $h_z = H_z/[2S(D-|E|)]$. If transverse anisotropies are distributed the magnetization relaxation curve in the Arrhenius regime is given by

$$R(t) = 2\int_0^\infty dE f_E(E) \exp[-\Gamma(E)t], \qquad (94)$$

where

$$\Gamma(E) = \Gamma_0 e^{-U(E)/T}. \qquad (95)$$

The transverse-anisotropy distribution $f_E(E)$ has been calculated in Sec. IV for a random array of linear dislocations. Using the results of that section, one can rewrite $R(t)$ in the scaling form

$$R(\tilde{t}) = 2\int_0^\infty d\alpha f_\alpha(\alpha) \exp[-\tilde{t}e^{p\alpha}], \qquad (96)$$

where $\tilde{t} \equiv t/\tau$, $\tau^{-1} = \Gamma_0 e^{-U_0/T}$, and

$$p \equiv \frac{1+h_z}{1-h_z}\frac{2U_0\tilde{E}_c}{T}. \qquad (97)$$

If $p \to 0$ in Eq. (96), then one returns to the simple exponential relaxation, $R(\tilde{t}) = \exp(-\tilde{t})$. In the case of $p \gg 1$ one has $R(\tilde{t}) \cong 2\int_0^{\alpha_t} d\alpha f_\alpha(\alpha)$, where $\alpha_t = (1/p)\ln(1/\tilde{t})$, i.e., relaxation is logarithmically stretched. For Mn_{12} in the kelvin range, U_0/T is large but the value of $\tilde{E}_c$ is small for a realistic concentration of dislocations c, so that p is typically of order unity. Using estimates from the final part of Sec. IV, at $H_z = 0$ and $T = 1$K one obtains $p = 1.94$ for $c = 10^{-2}$, $p = 0.61$ for $c = 10^{-3}$, and $p = 0.194$ for $c = 10^{-4}$. Thus Eq. (96) does not simplify and it should be computed numerically with the use of Eq. (47). Note that for large crystals f_α can be approximated by the Gaussian of Eq. (49), which implies that the actual parameter of the problem is $\tilde{p} = 2\sqrt{L}p \approx 6.5p$.

The short-time behavior of $R(\tilde{t})$ is singular due to Mn_{12} molecules [see Eq. (52)] which are close to dislocations. These molecules correspond to the asymptote of the anisotropy-distribution function, $f_\alpha \cong 1/\alpha^3$, for $\alpha \gtrsim \alpha_1$, which yields

$$R(\tilde{t}) \cong 1 - \left[\frac{p}{\ln(1/\tilde{t})}\right]^2. \qquad (98)$$

The singularity is rather weak for large crystals since the fraction n_1 of molecules which relax according to Eq. (98) is small. One can find the time $\tilde{t}_1$ at which this stage of relaxation is completed from the condition $R(\tilde{t}_1) = 1 - n_1$ that gives

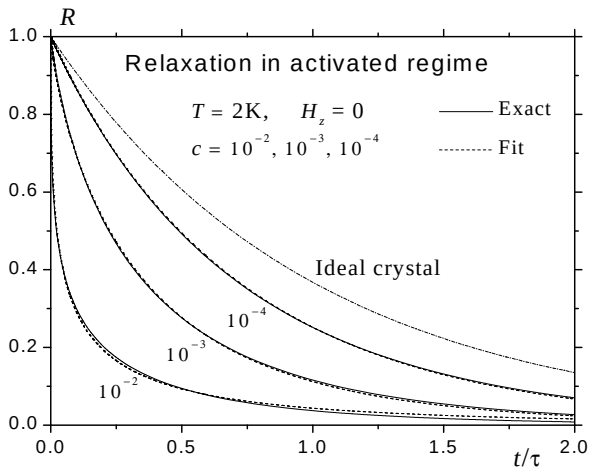

FIG. 14. Magnetization relaxation curves for Mn_{12} with dislocations in the activated regime. The fitted values of ζ decrease on lowering temperature and increasing c.

$$\tilde{t}_1 = \exp[-p/\sqrt{n_1}] = \exp\left[-p\sqrt{4L\ln(4L/\sqrt{\pi})}\right]. \quad (99)$$

It is exponentially small for $p \gg 1$ and/or for large crystals. If [see comment after Eq. (52)] one replaces α_1 by three $3\alpha_1$, the exponent of Eq. (99) will increase by a factor of three. This means that the actual value of t_1 is much smaller and the best way to find it is to compare Eq. (98) with the exact relaxation curve of Eq. (96). Note, however, that in natural units this time is $t_1 = \tau\tilde{t}_1$, where τ is the relaxation time of an ideal Mn_{12} crystal which is exponentially long for $p \gg 1$.

Numerically computed relaxation curves $R(\tilde{t})$ for $H_z = 0$, $T = 2$K, and different concentrations of dislocations c are shown in Fig. 14. One can see that deviations of $R(\tilde{t})$ from a pure exponential are quite pronounced. For not too large concentrations c one can fit $R(\tilde{t})$ by a stretched exponential

$$R(\tilde{t}) = \exp(-a\tilde{t}^{\zeta}). \quad (100)$$

Although this dependence does not follow from any theory, the fits are surprisingly good. It would be interesting to see if the fit of the relaxation curve with Eq. (100) provides the actual concentration of dislocations in a Mn_{12} crystal found by other methods. For this purpose, we listed the fitted values of a and ζ, together with the parameter p of Eq. (97), in Table I for Mn_{12} crystals of the typical size 0.5×0.5 mm^2 at $T = 2$K and $H_z = 0$. For other temperatures and magnetic fields, one can interpolate a and ζ on p using Table I. Note that in our picture the $\exp(-\sqrt{t})$ relaxation observed in some experiments is one of many possibilities corresponding to different fields, temperatures, and concentrations.

TABLE I. Parameter p of Eq. (97) and fitting parameters a and ζ for 0.5×0.5 mm^2 Mn_{12} crystals at $T = 2$K, $H_z = 0$, and different concentrations of dislocations c.

c	p	a	ζ
10^{-4}	0.097	1.38	0.97
3×10^{-4}	0.168	1.68	0.91
10^{-3}	0.306	2.19	0.77
3×10^{-3}	0.530	2.68	0.59
10^{-2}	0.97	3.13	0.40

IX. CONCLUSIONS

We have developed a comprehensive theory of quantum spin relaxation in Mn_{12} acetate crystals, which takes into account imperfections of the crystal structure and is based upon the generalization of the Landau-Zener effect for incoherent tunneling from excited energy levels. All experimental features of the low-temperature magnetic behavior of Mn_{12} crystals find natural explanation within this theoretical framework.

Linear dislocations at plausible concentrations provide the transverse anisotropy which is the main source of tunneling in Mn_{12}. Local rotations of the easy axis due to dislocations result in a transverse magnetic field for any external field applied along the c-axis of the crystal. For odd resonances, the tunneling matrix element contains the transverse field only in the first order of the perturbation theory, while the tranverse anisotropy makes the principal contribution to the transition amplitude. This explains the presence of odd tunneling resonances and their strength relative to that of even resonances.

Transverse anisotropies and fields are distributed in the crystal. One consequence of that distribution is that the temperature of the crossover between quantum and thermal behavior becomes distributed within an appreciable range. This may be in part responsible for the experimental fact that quantum steps in the hysteresis of Mn_{12} are well pronounced in the thermally activated regime.

Crystal defects produce a broad distribution of tunnel splittings that can be extracted from the dependence of the magnetic relaxation on the field-sweep rate. The theory predicts that relaxation curves for different tunneling resonances can be scaled onto one master curve.[58] The first derivative of this curve equals the distribution function of transverse anisotropies in the crystal.

Due to that distribution, quantum steps in the magnetization curve should appear and disappear in a peculiar manner. At a given temperature and field-sweep rate, our theory predicts which steps must be absent[58] regardless of the distribution function.

Another consequence of the distribution is that the magnetic relaxation in the thermally activated regime follows the stretched-exponential law. The exponent in this law depends on the field, temperature and concentration of defects. In zero field at $T = 2$K it is between 0.97 and 0.40 for concentrations ranging from 10^{-4} to 10^{-2} per unit cell of the crystal.

ACKNOWLEDGMENTS

We thank Myriam Sarachik and members of her experimental group for numerous illuminating discussions and

for providing us with unpublished experimental data on Mn_{12}. This work has been supported by the NSF Grant No. 9978882.

[1] T. Lis, Acta Crystallogr. B **36**, 2042 (1980).
[2] M. Hennion, L. Pardi, I. Mirebeau, E. Suard, R. Sessoli, and A. Caneschi, Phys. Rev. B **56**, 8819 (1997).
[3] R. Sessoli, D. Gatteschi, A. Caneschi, and M. A. Novak, Nature (London) **365**, 141 (1993).
[4] R. Sessoli, Mol. Cryst. Liq. Crist. **274**, [801]/145 (1995).
[5] M. A. Novak and R. Sessoli, in *Quantum Tunneling of Magnetization*, edited by L. Gunther and B. Barbara (Kluwer, Dordrecht, 1995).
[6] J. R. Friedman, M. P. Sarachik, J. Tejada, and R. Ziolo, Phys. Rev. Lett. **76**, 3830 (1996).
[7] J. M. Hernández, X. X. Zhang, F. Luis, J. Bartolomé, J. Tejada, and R. Ziolo, Europhys. Lett. **35**, 301 (1996).
[8] L. Thomas, F. Lionti, R. Ballou, D. Gatteschi, R. Sessoli, and B. Barbara, Nature **383**, 145 (1996).
[9] W. Wernsdorfer, R. Sessoli, and D. Gatteschi, Europhys. Lett. **47**, 254 (1999).
[10] J. A. A. J. Perenboom, J. S. Brooks, S. Hill, T. Hathaway, and N. S. Dalal, Phys. Rev. B **58**, 330 (1998).
[11] L. Bokacheva, A. D. Kent, and M. A. Walters, Phys. Rev. Lett. **85**, 4803 (2000).
[12] A. D. Kent, Y. Zhong, L. Bokacheva, D. Ruiz, D. N. Hendrickson, and M. P. Sarachik, Europhys. Lett. **49**, 521 (2000).
[13] D. A. Garanin and E. M. Chudnovsky, Phys. Rev. B **56**, 11 102 (1997).
[14] E. M. Chudnovsky and D. A. Garanin, Phys. Rev. Lett. **79**, 4469 (1997).
[15] D. A. Garanin, X. Martínes Hidalgo, and E. M. Chudnovsky, Phys. Rev. B **57**, 13639 (1998).
[16] J.-Q. Liang, H. J. W. Müller-Kirsten, D.-K. Park, and F. Zimmerschied, Phys. Rev. Lett. **81**, 216 (1998).
[17] S.-Y. Lee, H. J. W. Müller-Kirsten, D.-K. Park, and F. Zimmerschied, Phys. Rev. B **58**, 5554 (1998).
[18] Y.-B. Zhang, J.-Q. Liang, H. J. W. Müller-Kirsten, S.-P. Kou, X.-B. Wang, and F.-C. Pu, Phys. Rev. B **60**, 12886 (1999).
[19] G.-H. Kim, Phys. Rev. B **59**, 11847 (1999).
[20] D. A. Garanin and E. M. Chudnovsky, Phys. Rev. B **59**, 3671 (1999).
[21] D. A. Garanin and E. M. Chudnovsky, Phys. Rev. B **63**, 024418 (2000).
[22] C.-S. Park, S.-K. Yoo, and D.-H. Yoon, Phys. Rev. B **61**, 11618 (2000).
[23] T. Choi and G.-H. Kim, Physica B **291**, 219 (2000).
[24] X. Martínes Hidalgo and E. M. Chudnovsky, J. Phys.: Condensed Matter **12**, 4243 (2000).
[25] J. R. Friedman, M. P. Sarachik, J. M. Hernández, X. X. Zhang, J. Tejada, E. Molins, and R. Ziolo, J. Appl. Phys. **81**, 3978 (1997).
[26] F. Luis, J. Bartolomé, J. F. Fernández, J. Tejada, J. M. Hernández, X. X. Zhang, and R. Ziolo, Phys. Rev. B **55**, 11448 (1997).
[27] J. R. Friedman, M. P. Sarachik, and R. Ziolo, Phys. Rev. B **58**, R14 729 (1998).
[28] A. Fort, A. Rettori, J. Villain, D. Gatteschi, and R. Sessoli, Phys. Rev. Lett. **80**, 612 (1998).
[29] A. M. Gomes, M. A. Novak, R. Sessoli, A. Caneschi, and D. Gatteschi, Phys. Rev. B **57**, 5021 (1998).
[30] L. Thomas, A. Caneschi, and B. Barbara, Phys. Rev. Lett. **83**, 2398 (1999).
[31] Y. Zhong, M. P. Sarachik, J. Yoo, and D. N. Hendrickson, Phys. Rev. B **62**, R9256 (2000).
[32] I. Chiorescu, R. Giraud, A. G. M. Jansen, A. Caneschi, and B. Barbara, Phys. Rev. Lett. **85**, 4807 (2000).
[33] J. Villain, A. Würger, A. Fort, and A. Rettori, J. Phys. I (France) **7**, 1583 (1997).
[34] M. N. Leuenberger and D. Loss, Europhys. Lett. **46**, 692 (1999).
[35] M. N. Leuenberger and D. Loss, Phys. Rev. B **61**, 1286 (2000).
[36] L. D. Landau, Phys. Z. Sowjetunion **2**, 46 (1932).
[37] C. Zener, Proc. R. Soc. London A **137**, 696 (1932).
[38] V. V. Dobrovitsky and A. K. Zvezdin, Europhys. Lett. **38**, 377 (1997).
[39] L. Gunther, Europhys. Lett. **39**, 1 (1997).
[40] M. N. Leuenberger and D. Loss, Phys. Rev. B **61**, 12200 (2000).
[41] E. M. Chudnovsky and D. A. Garanin (submitted, cond-mat/0105195).
[42] F. Hartmann-Boutron, P. Politi, and J. Villain, Int. J. Mod. Phys. B **10**, 2577 (1996).
[43] N. V. Prokof'ev and P. C. E. Stamp, Phys. Rev. Lett. **80**, 5794 (1998).
[44] D. A. Garanin, E. M. Chudnovsky, and R. Schilling, Phys. Rev. B **61**, 12204 (2000).
[45] E. M. Chudnovsky, Phys. Rev. Lett. **84**, 5676 (2000).
[46] N. V. Prokof'ev and P. C. E. Stamp, Phys. Rev. Lett. **84**, 5677 (2000).
[47] W. Wernsdorfer, C. Paulsen, and R. Sessoli, Phys. Rev. Lett. **84**, 5678 (2000).
[48] S. Miyashita and K. Saito (to be published).
[49] E. M. Chudnovsky and D. A. Garanin, Europhys. Lett. **52**, 245 (2000).
[50] M. N. Leuenberger and D. Loss, Europhys. Lett. **52**, 247 (2000).
[51] L. D. Landau and E. M. Lifshitz, *Theory of Elasticity* (Pergamon, New York, 1970).
[52] E. M. Chudnovsky and J. R. Friedman (unpublished).
[53] D. A. Garanin, J. Phys. A **24**, L61 (1991).
[54] A. Garg, Europhys. Lett. **22**, 205 (1993).
[55] E. Kececioglu and A. Garg, Phys. Rev. B **63**, 064422 (2001).
[56] D. A. Garanin (unpublished).
[57] W. Wernsdorfer and R. Sessoli, Science **284**, 133 (1999).
[58] This has been observed by M. P. Sarachik and K. Mertes (to be published).